MIMO Zero-Forcing Performance Evaluation Using the Holonomic Gradient Method

Constantin Siriteanu, Akimichi Takemura, Satoshi Kuriki, Hyundong Shin, Christoph Koutschan

***Abstract*—For multiple-input multiple-output (MIMO) spatial-multiplexing transmission, zero-forcing detection (ZF) is appealing because of its low complexity. Our recent MIMO ZF performance analysis for Rician–Rayleigh fading, which is relevant in heterogeneous networks, has yielded for the ZF outage probability and ergodic capacity infinite-series expressions. Because they arose from expanding the confluent hypergeometric function ${}_1F_1(\cdot,\cdot,\sigma)$ around 0, they do not converge numerically at realistically-high Rician K-factor values. Therefore, herein, we seek to take advantage of the fact that ${}_1F_1(\cdot,\cdot,\sigma)$ satisfies a differential equation, i.e., it is a *holonomic* function. Holonomic functions can be computed by the *holonomic gradient method* (HGM), i.e., by numerically solving the satisfied differential equation. Thus, we first reveal that the moment generating function (m.g.f.) and probability density function (p.d.f.) of the ZF signal-to-noise ratio (SNR) are holonomic. Then, from the differential equation for ${}_1F_1(\cdot,\cdot,\sigma)$, we deduce those satisfied by the SNR m.g.f. and p.d.f., and demonstrate that the HGM helps compute the p.d.f. accurately at practically-relevant values of K. Finally, numerical integration of the SNR p.d.f. output by the HGM yields accurate ZF outage probability and ergodic capacity results.**

***Index Terms*—Holonomic gradient method, hypergeometric function, MIMO, Rayleigh–Rician fading, zero-forcing.**

I. Introduction

A. Background

The performance of multiple-input multiple-output (MIMO) wireless communications systems has been attracting substantial interest [1] [2] [3] [4] [5]. Typically, its evaluation proceeds from expressions of performance measures — e.g., outage probability, ergodic capacity — derived based on statistical assumptions about the channel-fading matrix [1] [2] [4] [6] [7] [8].

For tractability, MIMO analyses have often assumed zero-mean channel matrix, i.e., Rayleigh fading [2]. However, state-of-the-art channel measurements and models, e.g., WINNER II [9], have revealed nonzero-mean channel, i.e., Rician fading [2]. MIMO performance analysis for Rician fading is much more complicated than for Rayleigh fading. Then, even for linear interference-mitigation approaches such as zero-forcing detection (ZF) and minimum mean-square error detection (MMSE) [10], the performance analysis of MIMO spatial-multiplexing transmission has been found tractable only for Rician–Rayleigh mixtures [4] [7].

ZF has been considered for WiMAX and LTE [11] and has recently been studied as relevant for distributed and large MIMO systems [5] [12] [13] [14] [15], mainly due to its low complexity. Nevertheless, although simple, for well-conditioned MIMO channel matrix, ZF approaches the performance of maximum-likelihood and minimum-error-rate (i.e., optimal) detection [16] [17] [18] [19]. Thus, the analysis of ZF performance for Rician fading has remained of interest — see [6] [7] and references therein.

B. Previous ZF Analyses

For perfectly-known uncorrelated Rayleigh fading channel, MIMO ZF performance was first characterized exactly in [20], by viewing ZF as the no-noise limit of optimum combining, i.e., MMSE [21, Remark 1]. Recently, though, it has been shown that performance measures for MMSE do not necessarily converge to those of ZF [22] [23] [24].

The results of [20] were extended to transmit-correlated fading in [25] [26] based on the fact that, given the channel matrix $\mathbf{H}$, the signal-to-noise ratio (SNR) for ZF is determined by matrix $\mathbf{H}^{\mathcal{H}}\mathbf{H}$, which is central-Wishart-distributed when $\mathbf{H}$ has zero mean and receive-correlation.

ZF has been studied for Rician fading, i.e., nonzero-mean $\mathbf{H}$, much less than for Rayleigh fading. This is because the analysis is complicated by the noncentral-Wishart distribution of $\mathbf{H}^{\mathcal{H}}\mathbf{H}$. Some approximation-based results for full-Rician fading have appeared for ZF in [6] and relevant references therein. (For MMSE, approximate and exact analyses under Rician–Rayleigh fading mixtures appeared in [21] and [4], respectively.)

Note that, although such fading mixtures have mainly been considered because they promote analysis tractability, they are nevertheless relevant in macrocells, microcells, and heterogeneous networks — see [4] [7] and references therein.

Thus, we have also analyzed ZF for such fading mixtures in [7] [8]. For the case when the intended stream undergoes Rician fading whereas the interfering streams undergo Rayleigh fading, [7] derived exact infinite-series expressions for ZF performance measures, and [8] proved their theoretical convergence.

C. Siriteanu is with the Department of Information Systems Engineering, Graduate School of Information Science and Technology, Osaka University.

A. Takemura is with the Department of Mathematical Informatics, Graduate School of Information Science and Technology, University of Tokyo, Japan, and Japan Science and Technology Agency, CREST.

S. Kuriki is with the Institute of Statistical Mathematics, Tachikawa, Tokyo, Japan.

H. Shin is with the Department of Electronics and Radio Engineering, Kyung Hee University, South Korea.

C. Koutschan is with the Johann Radon Institute for Computational and Applied Mathematics, Austrian Academy of Sciences, Linz, Austria.

C. Previous Approach and its Limitations. Motivation of New Approach.

The exact ZF analysis procedure we employed in [7] is as follows. First, we expressed, in [7, Eq. (31)], the moment generating function (m.g.f.) of the SNR for Rician-fading Stream 1 in terms of the confluent hypergeometric function ${}_1F_1(\cdot,\cdot,\sigma)$ [27, Ch. 13]. Then, the well-known expansion of ${}_1F_1(\cdot,\cdot,\sigma)$ around 0 from [27, Eq. (13.2.2), p. 322] yielded the infinite series for the SNR m.g.f. from [7, Eq. (37)]. Upon inverse-Laplace transformation, the latter yielded the infinite-series expression for the SNR probability density function (p.d.f.) from [7, Eq. (39)]. Finally, integration of this p.d.f. expression yielded the infinite-series expressions for ZF outage probability and ergodic capacity from [7, Eqs. (69), (71)].

However, as revealed in [7] [8], the computation of infinite series [7, Eqs. (39), (69), (71)] breaks down at much smaller Rician K-factor values than those considered realistic (e.g., averages of lognormal distributions proposed by WINNER II for K in [9]). This is the consequence of the employed expansion of ${}_1F_1(\cdot,\cdot,\sigma)$, whose own computation away from $\sigma = 0$ is nontrivial: with increasing σ, numerical convergence is increasingly difficult (i.e., slow, resource-intensive) and eventually fails [28] [29] [30] [31]. Note that hypergeometric functions[1] and infinite-series expressions have been found to characterize the performance for many other MIMO techniques under many fading types [2] [4] [30] [31] [32]. Limitations in computing these infinite-series for MIMO evaluation motivates our search herein for an alternative approach.

D. New Approach and Contribution

A seldom-considered approach for computing ${}_1F_1(\cdot,\cdot,\sigma)$ follows from the fact that it satisfies, with respect to (w.r.t.) σ, a linear differential equation with polynomial coefficients [27, Eq. (13.2.1), p. 322], i.e., this function is *holonomic* [33, p. 334] [34, p. 7] [35, p. 140] [36, Section 6.4]. Any holonomic function can be computed at some σ by numerically solving its differential equation starting from some σ_0 where the function is either known analytically or can be approximated accurately.

The computation of a holonomic function by numerically solving satisfied differential equations is known as the *holonomic gradient method* (HGM) [37] [38]. It has recently been applied in statistics to evaluating the normalizing constant of the Bingham distribution [37] and the cumulative distribution function (c.d.f.) of the dominant eigenvalue of a real-valued Wishart-distributed matrix [38], upon deriving relevant differential equations. To the best of our knowledge, the HGM has not yet been applied for MIMO performance evaluation, although MIMO performance measures have often been expressed in terms of holonomic special functions and ensuing infinite series [2] [31] [32] [28] [7] — see also [30] and references therein.

The current paper proposes the HGM-based evaluation of the exact MIMO ZF performance under Rician–Rayleigh fading. Starting from the ZF SNR m.g.f. expression derived in terms of ${}_1F_1(\cdot,\cdot,\sigma)$ in [7, Eq. (31)] and the differential equation satisfied by ${}_1F_1(\cdot,\cdot,\sigma)$ [27, Eq. (13.2.1), p. 322], we first deduce for the SNR m.g.f. the satisfied differential equations. Their inverse-Laplace transformation yields for the SNR p.d.f. the satisfied differential equations.

These are shown to enable the accurate HGM-based computation of the SNR p.d.f. at practical K values, starting from an initial value computed by truncating the available infinite-series p.d.f. expression from [7, Eq. (39)]. Furthermore, numerical integration of the HGM output (i.e., the SNR p.d.f.) yields accurately, for the first time, the outage probability and ergodic capacity for MIMO ZF at K values relevant to WINNER II.

The HGM-based approach is envisioned to lead to a new framework for the analysis and evaluation of MIMO under general fading. As the complexity of MIMO analyses seeking explicit performance measure expressions has been increasing, an ability to derive (perhaps automatically) differential equations for MIMO performance measures and to compute them by the HGM may be a more general, more straightforward, and more effective alternative.

E. Notation

The notation defined below follows closely that from [7]. Thus, scalars, vectors, and matrices are represented with lowercase italics, lowercase boldface, and uppercase boldface, respectively, e.g., a, $\mathbf{h}$, and $\mathbf{H}$; superscripts $\cdot^{\mathcal{T}}$ and $\cdot^{\mathcal{H}}$ stand for transpose and Hermitian (i.e., complex-conjugate) transpose; $[\cdot]_{i,j}$ indicates the i,jth element of a matrix; $\|\mathbf{H}\|^2 = \sum_i^{N_\mathrm{R}} \sum_j^{N_\mathrm{T}} |[\mathbf{H}]_{i,j}|^2$ is the squared Frobenius norm of $N_\mathrm{R} \times N_\mathrm{T}$ matrix $\mathbf{H}$; $\propto$ stands for 'proportional to'; subscripts $\cdot_\mathrm{d}$ and $\cdot_\mathrm{r}$ identify, respectively, the deterministic and random components; subscript $\cdot_\mathrm{n}$ indicates a normalized variable; $\mathbb{E}\{\cdot\}$ denotes statistical average; $(N)_n$ is the Pochhammer symbol, i.e., $(N)_0 = 1$ and $(N)_n = N(N+1)\ldots(N+n-1)$, $\forall n > 1$ [27, p. xiv], and ${}_1F_1(\cdot;\cdot;\cdot)$ is the confluent hypergeometric function [27, Eq. (13.2.2), p. 322].

F. Paper Organization

Section II describes the MIMO signal, noise, and channel models. Section III introduces the ZF SNR m.g.f. and p.d.f. infinite-series expressions derived in [7], and discusses difficulties encountered in the computation of the infinite-series expression for the SNR-p.d.f. and ensuing performance measures. Section IV defines holonomic functions and deduces from their properties that the SNR m.g.f. and p.d.f. are holonomic. This justifies our search in Section V for the differential equations they satisfy. These differential equations are then exploited using the HGM to generate the numerical results shown and discussed in Section VI. Finally, Section VII discusses other possible HGM applications in MIMO evaluation.

II. Signal, Noise, and Fading Models

Herein, the signal, noise, and channel models and assumptions follow closely the ones from [7]. Thus, we consider uncoded MIMO spatial-multiplexing over a frequency-flat

[1] Of both scalar and matrix arguments.

fading channel and assume that there are N_T and N_R antenna elements at the transmitter(s) and receiver, respectively, with $N_\mathrm{T} \leq N_\mathrm{R}$. Let us denote the number of degrees of freedom as

$$N = N_\mathrm{R} - N_\mathrm{T} + 1. \tag{1}$$

Letting $\mathbf{x} = [x_1\, x_2\, \cdots\, x_{N_\mathrm{T}}]^{\mathcal{T}}$ denote the $N_\mathrm{T} \times 1$ zero-mean transmit-symbol vector with $\mathbb{E}\{\mathbf{x}\mathbf{x}^{\mathcal{H}}\} = \mathbf{I}_{N_\mathrm{T}}$, the $N_\mathrm{R}\times 1$ vector with the received signals can be represented as [1, Eq. (8)] [7, Eq. (1)]:

$$\mathbf{r} = \sqrt{\frac{E_\mathrm{s}}{N_\mathrm{T}}}\,\mathbf{H}\mathbf{x} + \mathbf{v} = \sqrt{\frac{E_\mathrm{s}}{N_\mathrm{T}}}\,\mathbf{h}_1 x_1 + \sqrt{\frac{E_\mathrm{s}}{N_\mathrm{T}}}\sum_{k=2}^{N_\mathrm{T}} \mathbf{h}_k x_k + \mathbf{v}. \tag{2}$$

Above, $E_\mathrm{s}/N_\mathrm{T}$ represents the energy transmitted per symbol (i.e., per antenna), so that E_s is the energy transmitted per channel use. The additive noise vector $\mathbf{v}$ is zero-mean, uncorrelated, circularly-symmetric complex-valued Gaussian [1] with variance N_0 per dimension. We will also employ its normalized version $\mathbf{v}_\mathrm{n} = \mathbf{v}/\sqrt{N_0}$. We shall employ the per-symbol input SNR, defined as

$$\Gamma_\mathrm{s} = \frac{E_\mathrm{s}}{N_0}\frac{1}{N_\mathrm{T}}, \tag{3}$$

as well as the per-bit input SNR, which, for a modulation constellation with M symbols (e.g., MPSK), is defined as

$$\Gamma_\mathrm{b} = \frac{\Gamma_\mathrm{s}}{\log_2 M}. \tag{4}$$

Then, $\mathbf{H} = (\mathbf{h}_1\ \mathbf{h}_2\ \ldots\ \mathbf{h}_{N_\mathrm{T}})$ is the $N_\mathrm{R} \times N_\mathrm{T}$ complex-Gaussian channel matrix. Vector $\mathbf{h}_k$ comprises the channel factors between transmit-antenna k and all receive-antennas. The deterministic (i.e., mean) and random components of $\mathbf{H}$ are denoted as $\mathbf{H}_\mathrm{d} = (\mathbf{h}_{\mathrm{d},1}\ \mathbf{h}_{\mathrm{d},2}\ \ldots\ \mathbf{h}_{\mathrm{d},N_\mathrm{T}})$ and $\mathbf{H}_\mathrm{r} = (\mathbf{h}_{\mathrm{r},1}\ \mathbf{h}_{\mathrm{r},2}\ \ldots\ \mathbf{h}_{\mathrm{r},N_\mathrm{T}})$, respectively, so that $\mathbf{H} = \mathbf{H}_\mathrm{d} + \mathbf{H}_\mathrm{r}$. If $[\mathbf{H}_\mathrm{d}]_{i,j} = 0$ then $|\,[\mathbf{H}]_{i,j}\,|$ has a Rayleigh distribution; otherwise, $|\,[\mathbf{H}]_{i,j}\,|$ has a Rician distribution [2]. Typically, the channel matrix for Rician fading is written as [1]

$$\mathbf{H} = \mathbf{H}_\mathrm{d} + \mathbf{H}_\mathrm{r} = \sqrt{\frac{K}{K+1}}\,\mathbf{H}_\mathrm{d,n} + \sqrt{\frac{1}{K+1}}\,\mathbf{H}_\mathrm{r,n}, \tag{5}$$

where, for normalization purposes [39], it is assumed that

$$\|\mathbf{H}_\mathrm{d,n}\|^2 = \mathbb{E}\{\|\,[\mathbf{H}_\mathrm{r,n}]\,\|^2\} = N_\mathrm{T}N_\mathrm{R}, \tag{6}$$

so that $\mathbb{E}\{\|\mathbf{H}\|^2\} = N_\mathrm{T}N_\mathrm{R}$. Power ratio

$$K = \frac{\|\mathbf{H}_\mathrm{d}\|^2}{\mathbb{E}\{\|\mathbf{H}_\mathrm{r}\|^2\}} = \frac{\frac{K}{K+1}\|\mathbf{H}_\mathrm{d,n}\|^2}{\frac{1}{K+1}\mathbb{E}\{\|\mathbf{H}_\mathrm{r,n}\|^2\}} \tag{7}$$

is the Rician K-factor: $K = 0$ yields Rayleigh fading for all elements of $\mathbf{H}$; $K \neq 0$ yields Rician fading if $\mathbf{H}_\mathrm{d,n} \neq \mathbf{0}$.

In [7], we partitioned into the column with the fading gains that affect the intended stream, i.e., Stream 1, and the matrix columns with the fading gains that affect the interfering streams, i.e.,

$$\mathbf{H} = (\mathbf{h}_1\ \ \mathbf{H}_2) = (\mathbf{h}_{\mathrm{d},1}\ \ \mathbf{H}_{\mathrm{d},2}) + (\mathbf{h}_{\mathrm{r},1}\ \ \mathbf{H}_{\mathrm{r},2}), \tag{8}$$

and assumed, for analysis tractability, that $\mathbf{h}_{\mathrm{d},1} \neq \mathbf{0}$ and $\mathbf{H}_{\mathrm{d},2} = \mathbf{0}$, i.e., Rician–Rayleigh fading. Then, we can write

$$\begin{aligned}\|\mathbf{h}_{\mathrm{d},1}\|^2 &= \|(\mathbf{h}_{\mathrm{d},1}\ \ \mathbf{0}_{N_\mathrm{R}\times(N_\mathrm{T}-1)})\|^2 = \|\mathbf{H}_\mathrm{d}\|^2 \\ &= \frac{K}{K+1}N_\mathrm{R}N_\mathrm{T}.\end{aligned} \tag{9}$$

As in [25] [26], for tractability, we assume zero receive-correlation and we allow for nonzero transmit-correlation whereby all conjugate-transposed rows of $\mathbf{H}_\mathrm{r,n}$ have distribution $\mathcal{CN}(\mathbf{0}, \mathbf{R}_\mathrm{T})$. Consequently, all conjugate-transposed rows of $\mathbf{H}_\mathrm{r}$ have distribution $\mathcal{CN}(\mathbf{0}, \mathbf{R}_{\mathrm{T},K} = \frac{1}{K+1}\mathbf{R}_\mathrm{T})$.

It can be shown that normalization $\mathbb{E}\{\|\,[\mathbf{H}_\mathrm{r,n}]\,\|^2\} = N_\mathrm{T}N_\mathrm{R}$ is equivalent with

$$\sum_{i=1}^{N_\mathrm{T}} [\mathbf{R}_\mathrm{T}]_{i,i} = N_\mathrm{T}. \tag{10}$$

Because the diagonal elements of $\mathbf{R}_\mathrm{T}$ need not be equal, our analysis applies also for distributed transmitters. Nevertheless, for simplicity, numerical results are shown herein only for the case $[\mathbf{R}_\mathrm{T}]_{i,i} = 1$, $\forall i$, i.e., for collocated transmitters.

The elements of $\mathbf{R}_\mathrm{T}$ can be computed from the azimuth spread (AS) as shown in [6, Section VI.A] for WINNER II, i.e., Laplacian, power azimuth spectrum. Note that WINNER II has modeled both K (in dB) and AS (in degrees) as random variables with scenario-dependent lognormal distributions [9]. Herein, we show results for K and AS set to their averages for WINNER II indoor scenario A1.

III. Infinite-Series Expressions for MIMO ZF SNR M.G.F. and P.D.F.

A. MIMO ZF and Its SNR M.G.F. for Rician–Rayleigh Fading

For the received-signal vector from (2), ZF means mapping the elements of the following vector into the closest modulation constellation symbols [1, Eq. (22)]:

$$\sqrt{\frac{N_\mathrm{T}}{E_\mathrm{s}}}\left[\mathbf{H}^{\mathcal{H}}\mathbf{H}\right]^{-1}\mathbf{H}^{\mathcal{H}}\,\mathbf{r} = \mathbf{x} + \frac{1}{\sqrt{\Gamma_\mathrm{s}}}\left[\mathbf{H}^{\mathcal{H}}\mathbf{H}\right]^{-1}\mathbf{H}^{\mathcal{H}}\mathbf{v}_\mathrm{n}. \tag{11}$$

Then, the ZF SNR for Stream 1 is given by

$$\gamma_1 = \frac{\Gamma_\mathrm{s}}{[(\mathbf{H}^{\mathcal{H}}\mathbf{H})^{-1}]_{1,1}}. \tag{12}$$

Its m.g.f. is defined as [2, Eq. (1.2)]

$$M_{\gamma_1}(s) = \mathbb{E}\{e^{s\gamma_1}\} = \int_0^\infty e^{st}p_{\gamma_1}(t)\mathrm{d}t, \tag{13}$$

where $\mathbb{E}\{\cdot\}$ stands for mean, and $p_{\gamma_1}(t,a)$ is the p.d.f. of γ_1. Thus, the m.g.f. is related to the Laplace transform [27, Eq. (1.14.17)] $L_{\gamma_1}(s,a)$ of the p.d.f. simply by a sign change, i.e.,

$$M_{\gamma_1}(-s) = L_{\gamma_1}(s) = \int_0^\infty e^{-st}p_{\gamma_1}(t)\mathrm{d}t. \tag{14}$$

If we define as in [7, Eqs. (18), (23)], respectively,

$$\Gamma_1 = \frac{\Gamma_\mathrm{s}}{\left[\mathbf{R}_{\mathrm{T},K}^{-1}\right]_{1,1}} \propto \frac{\Gamma_\mathrm{s}}{K+1}, \tag{15}$$

$$a = \left[\mathbf{R}_{\mathrm{T},K}^{-1}\right]_{1,1}\|\mathbf{h}_{\mathrm{d},1}\|^2 \propto KN_\mathrm{R}N_\mathrm{T}, \tag{16}$$

then, for MIMO ZF under Rician–Rayleigh fading, we can write the following exact expression for the m.g.f. of the SNR of the Rician-fading Stream 1 [7, Eq. (31)]:

$$M_{\gamma_1}(s,a) = \frac{1}{(1-\Gamma_1 s)^N}\,{}_1F_1\left(N; N_{\mathrm{R}}; a\frac{\Gamma_1 s}{1-\Gamma_1 s}\right), \quad (17)$$

where ${}_1F_1(N; N_{\mathrm{R}}; \sigma)$ is the confluent hypergeometric function of scalar argument σ [27, Ch. 13].

Remark 1: We have added a as variable for the SNR m.g.f. in (17) because, for Rayleigh-only fading, $a = 0$ (because $K = 0$), whereas, for Rician fading, $a \neq 0$ and increases with K. Thus, variable a is required later for HGM-based computation of the SNR p.d.f., using differential equations deduced from (17).

B. Infinite Series for SNR M.G.F. and P.D.F. for Rician–Rayleigh Fading

The confluent hypergeometric function is well-known to satisfy the infinite-series expression [27, Eq. (13.2.2), p. 322]

$${}_1F_1(N; N_{\mathrm{R}}; \sigma) = \sum_{n=0}^{\infty} \frac{(N)_n}{(N_{\mathrm{R}})_n}\frac{\sigma^n}{n!} = \sum_{n=0}^{\infty} A_n(\sigma). \quad (18)$$

One can readily show that the infinite-series expression (18) is the expansion around $\sigma = 0$ of ${}_1F_1(N; N_{\mathrm{R}}; \sigma)$, by using an integral expression for ${}_1F_1(N; N_{\mathrm{R}}; \sigma)$, as in [27, Eq. (13.4.1), p. 326] [27, Eq. (13.6.1), p. 327].

Using (18), we rewrote (17) in [7, Eq. (37)] as the infinite series

$$M_{\gamma_1}(s,a) = \sum_{n=0}^{\infty} A_n(a) \sum_{m=0}^{n} \binom{n}{m} \frac{(-1)^m}{(1-s\Gamma_1)^{N+n-m}}. \quad (19)$$

Its inverse-Laplace transformation has yielded for the SNR p.d.f. the infinite series[2] [7, Eq. (39)]

$$\begin{aligned} p_{\gamma_1}(t,a) &= \sum_{n=0}^{\infty} A_n(a) \sum_{m=0}^{n} \binom{n}{m} \\ &\quad \times \frac{(-1)^m t^{N+n-m-1} e^{-t/\Gamma_1}}{[(N+n-m)-1]!\,\Gamma_1^{N+n-m}}. \end{aligned} \quad (20)$$

For the outage probability and ergodic capacity (in bits per channel use — bpcu), which are defined as[3]

$$P_{\mathrm{o}}(\gamma_{1,\mathrm{th}}, a) = \text{Probability}(\gamma_1 \leq \gamma_{1,\mathrm{th}}) = \int_0^{\gamma_{1,\mathrm{th}}} p_{\gamma_1}(t,a)\mathrm{d}t, \quad (21)$$

$$C(a) = \mathbb{E}_{\gamma_1}\{C(\gamma_1, a)\} = \int_0^{\infty} \log_2(1+t) p_{\gamma_1}(t,a)\mathrm{d}t. \quad (22)$$

analytical integration of the infinite-series p.d.f. expression (20) has yielded the infinite-series expressions in [7, Eqs. (69), (71)], respectively.

[2]Note that, for $K \neq 0$, i.e., for Rician–Rayleigh fading, (19) and (20) reveal that the distribution of the ZF SNR is an infinite linear combination of Gamma distributions.

[3]In (21), $\gamma_{1,\mathrm{th}}$ is the threshold SNR.

C. Expressions for Rayleigh-Only Fading

For the special case of Rayleigh-only fading, because $a = 0$, only the term for $n = m = 0$ remains in (19) and (20), i.e.,

$$M_{\gamma_1}(s,0) = \frac{1}{(1-s\Gamma_1)^N}, \quad (23)$$

$$p_{\gamma_1}(t,0) = \frac{t^{N-1}e^{-t/\Gamma_1}}{(N-1)!\,\Gamma_1^N}, \quad t \geq 0, \quad (24)$$

so that the ZF SNR is Gamma-distributed [25] [26]. Then, (21) and (22) yield[4]

$$P_{\mathrm{o}}(\gamma_{1,\mathrm{th}}, 0) = \frac{1}{(N-1)!\Gamma_1^N}\int_0^{\gamma_{1,\mathrm{th}}} t^{N-1}e^{-t/\Gamma_1}\mathrm{d}t, \quad (25)$$

$$C(0) = \frac{1}{\ln 2}\frac{1}{(N-1)!}\frac{1}{\Gamma_1^N}\int_0^{\infty} \ln(1+t)t^{N-1}e^{-t/\Gamma_1}\mathrm{d}t. \quad (26)$$

D. Difficulties Computing the Derived Infinite Series

As mentioned in the Introduction, we proved analytically in [8] that the infinite series (20), along with the ensuing infinite series for the outage probability and ergodic capacity, converge everywhere. However, they cannot be computed (by truncation) accurately, or even at all, with increasing K — see [7, Sections V.F, VI.C] [8] for discussion and results.

This limitation is also illustrated herein for the SNR p.d.f. infinite series in (20) in Fig. 1, for $N_{\mathrm{R}} = 6$, $N_{\mathrm{T}} = 2$. We have set $K = 7$ dB and AS $= 51°$, i.e., the average K and AS for WINNER II scenario A1 (indoor office/residential) [6, Table I] [9]. On one hand, results for Rayleigh-only fading (identified in legend with `Ray–Ray`) reveal agreement between expression (24) and Monte Carlo simulation. On the other hand, for Rician–Rayleigh fading (identified in legend with `Rice–Ray`), the results from series (20) cannot even be plotted. In fact, for $N_{\mathrm{R}} = 6$ and $N_{\mathrm{T}} = 2$, we have been able to accurately compute $p_{\gamma_1}(t)$, and, thus, the outage probability and ergodic capacity, only up to $K \approx 1.5$ dB, as depicted in [8, Fig. 2]. This is because, by increasing K, i.e., a, we move σ further from the origin of expansion (18). We have also found that increasing N_{T} to 6 decreases the value of K that still yields accurate results to -3 dB [8, Figs. 1, 2], which is also explained by (16).

Since series truncation cannot help compute ZF performance measures for relevant SNR and parameter values, we pursue next an HGM-based approach.

IV. Holonomic Functions and the Holonomic Gradient Method (HGM)

A. Differential Equation for ${}_1F_1(N; N_R; \sigma)$

It is known that ${}_1F_1(N; N_{\mathrm{R}}; \sigma)$ satisfies the second-order ordinary differential equation with polynomial coefficients [27, Eq. (13.2.1), p. 322]

$$\begin{aligned} &\sigma \cdot {}_1F_1^{(2)}(N; N_{\mathrm{R}}; \sigma) + (N_{\mathrm{R}} - \sigma) \cdot {}_1F_1^{(1)}(N; N_{\mathrm{R}}; \sigma) \\ &\quad - N \cdot {}_1F_1(N; N_{\mathrm{R}}; \sigma) = 0, \end{aligned} \quad (27)$$

[4]The finite- and infinite-limit integrals involved in these expressions can be computed accurately numerically.

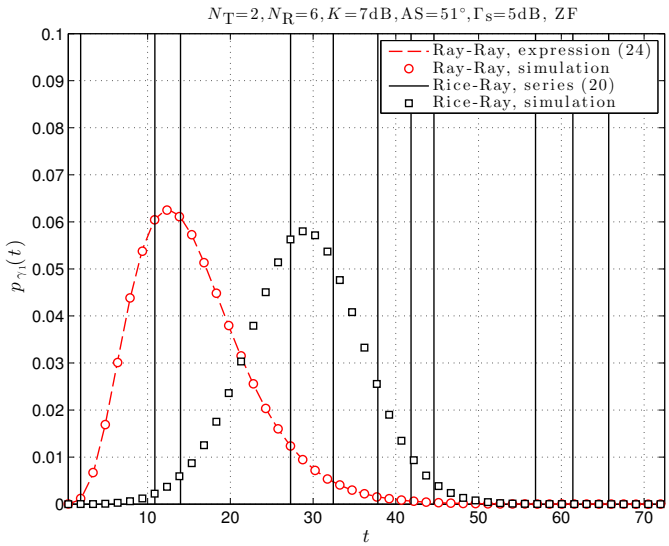

Fig. 1. P.d.f. of the SNR (in linear units) for Stream 1, for $N_R = 6$, $N_T = 2$, $K = 7$ dB, AS $= 51°$, $\Gamma_s = 5$ dB. For Rayleigh fading: from Monte Carlo simulation and expression (24). For Rician fading: from simulation and attempt to employ series (20); the latter produced the vertical black lines (which connect the points of extreme positive and negative values resulting from series truncation).

where ${}_1F_1^{(k)}(N; N_R; \sigma)$ stands for the kth derivative w.r.t. the sole variable σ.

In general, a function is called *holonomic* if it satisfies, w.r.t. each variable, an ordinary differential equation with polynomial coefficients [37, Section 2]. Thus, the confluent hypergeometric function ${}_1F_1(N; N_R; \sigma)$ is holonomic because it satisfies (27). Simpler examples of holonomic functions are the polynomial and exponential-polynomial functions [33, Section 2.5].

Let us now introduce the HGM-based computation of a holonomic function on the example of ${}_1F_1(N; N_R; \sigma)$. First, (27) can be recast as the system of differential equations

$$\partial_\sigma \begin{pmatrix} {}_1F_1(N; N_R; \sigma) \\ {}_1F_1^{(1)}(N; N_R; \sigma) \end{pmatrix} = \begin{pmatrix} 0 & 1 \\ \frac{N}{\sigma} & 1 - \frac{N_R}{\sigma} \end{pmatrix} \begin{pmatrix} {}_1F_1(N; N_R; \sigma) \\ {}_1F_1^{(1)}(N; N_R; \sigma) \end{pmatrix}.$$

If we denote as $\mathbf{f}(\sigma)$ the vector made of functions ${}_1F_1(N; N_R; \sigma)$ and ${}_1F_1^{(1)}(N; N_R; \sigma)$, and as $\mathbf{F}(\sigma)$ the 2×2 matrix on the right-hand side above, which is also known as the *companion* matrix, then, we have, more compactly,

$$\partial_\sigma \mathbf{f}(\sigma) = \mathbf{F}(\sigma)\mathbf{f}(\sigma), \tag{28}$$

whose left-hand side is the *gradient* of $\mathbf{f}(\sigma)$ w.r.t. σ.

B. HGM-Based Computation of Holonomic Function, e.g., ${}_1F_1(\cdot; \cdot; \sigma)$

Let us assume that initial conditions ${}_1F_1(N; N_R; \sigma_0)$ and ${}_1F_1^{(1)}(N; N_R; \sigma_0)$ are known for some σ_0. Then, ${}_1F_1(N; N_R; \sigma)$ can be computed for any σ by numerically solving[5] (28) between σ_0 and σ. Because σ appears in $\mathbf{F}(\sigma)$ denominators, one cannot use $\sigma_0 = 0$, for which it is known analytically, from (18) and [27, Eq. (13.3.15), p. 325], that ${}_1F_1(N; N_R; 0) = 1$ and ${}_1F_1^{(1)}(N; N_R; 0) = \frac{N}{N_R}$. Thus, initial conditions ${}_1F_1(N; N_R; \sigma_0)$ and ${}_1F_1^{(1)}(N; N_R; \sigma_0) = \frac{N}{N_R}\, {}_1F_1(N+1; N_R+1; \sigma_0)$ [27, Eq. (13.3.15), p. 325] have to be obtained numerically by truncation of series (18) for some $\sigma_0 > 0$. Nevertheless, since σ_0 can be selected arbitrarily small, highly-accurate computation of the initial condition $\mathbf{f}(\sigma_0)$ is possible based on the infinite-series expression of ${}_1F_1(N; N_R; \sigma)$.

The entire procedure is summarized below [37, Section 2.1]:

- First, compute accurate initial conditions, i.e., ${}_1F_1(N; N_R; \sigma_0)$ and ${}_1F_1^{(1)}(N; N_R; \sigma_0)$, for some sufficiently-small $\sigma_0 > 0$, by infinite-series truncation.
- Then, solve numerically the system of differential equations (28) between σ_0 and σ.

Such computation procedure (applicable to any holonomic function) is referred to as the *holonomic gradient method* [37] [38] (HGM) because, after starting from an initial condition, the *holonomic* function is computed by updating its *gradient*.

C. ZF SNR M.G.F. and P.D.F. Are Holonomic Functions

Holonomic functions satisfy the following properties:

- If $f(x)$ is a polynomial then $1/f(x)$ is holonomic [33, Prop. 2.1].
- If $f(x)$ is holonomic and $h(x)$ is rational then $f(h(x))$ is holonomic [34, Th. 1.4.2, p. 16].
- If $f(x)$ and $g(x)$ are holonomic then $f(x)\, g(x)$ is holonomic [33, Prop. 3.2].
- If $f(x)$ is holonomic then its Fourier transform is holonomic [33, p. 337].

Based on these properties, in the SNR m.g.f. expression from (17), the term $1/(1 - \Gamma_1 s)^N$ is holonomic w.r.t. s, and the term ${}_1F_1\left(N; N_R; a\frac{\Gamma_1 s}{1-\Gamma_1 s}\right)$ is holonomic w.r.t. s and a, yielding the following property.

Lemma 1: The SNR m.g.f. $M_{\gamma_1}(s, a)$ is holonomic w.r.t. both s and a, i.e., it must satisfy ordinary differential equations with polynomial coefficients w.r.t. both s and a. Also, the SNR p.d.f. $p_{\gamma_1}(t, a)$ is holonomic w.r.t. both t and a, i.e., it must satisfy ordinary differential equations with polynomial coefficients w.r.t. both t and a.

D. Proposed HGM-based ZF Performance Evaluation

The remainder of this work is devoted to applying HGM for ZF performance evaluation, as follows:

- Deduce the differential equations (known to exist) satisfied by $M_{\gamma_1}(s, a)$, w.r.t. both s and a, as well as by $p_{\gamma_1}(t, a)$, w.r.t. both t and a. This is necessary because, as we shall see, the partial derivatives are intertwined within differential equations w.r.t. s and a for $M_{\gamma_1}(s, a)$, i.e., w.r.t. t and a for $p_{\gamma_1}(t, a)$.
- Exploit the differential equations for the p.d.f. $p_{\gamma_1}(t, a)$ to accurately compute it by the HGM at practically-relevant values of K.
- Integrate numerically as in (21), (22) to compute the outage probability and ergodic capacity.

[5] E.g., with the `ode` function, in `MATLAB`.

V. Differential Equations for ZF SNR M.G.F. and P.D.F.

A. M.G.F. and P.D.F. Variable Scaling

In order to simplify notation and derivations hereafter, let us denote the m.g.f. $M_{\gamma_1}(s,a)$ and the p.d.f. $p_{\gamma_1}(t,a)$ for $\Gamma_1 = 1$ as $M(s,a)$ and $p(t,a)$, respectively. Now, by definition, we have

$$M(s,a) = \int_0^\infty e^{st} p(t,a) \mathrm{d}t. \tag{29}$$

Then, because

$$\begin{aligned} M_{\gamma_1}(s,a) &= M(s\Gamma_1, a) = \int_0^\infty e^{s\Gamma_1 t} p(t,a)\mathrm{d}t \\ &= \int_0^\infty e^{sy} \frac{1}{\Gamma_1} p\left(\frac{y}{\Gamma_1}, a\right) \mathrm{d}y, \end{aligned}$$

the p.d.f. $p_{\gamma_1}(t,a)$ of γ_1 for any Γ_1 can be obtained from $p(t,a)$ as follows:

$$p_{\gamma_1}(t,a) = \frac{1}{\Gamma_1} p\left(\frac{t}{\Gamma_1}, a\right). \tag{30}$$

Below, we first derive differential equations for $M(s,a)$ w.r.t. both s and a. From them we then deduce differential equations for $p(t,a)$ w.r.t. both t and a. They will help compute, by HGM, the function $p(t,a)$ at desired values of t and a (i.e., K). Finally, the transformation from (30) will return the value of the SNR p.d.f. $p_{\gamma_1}(t,a)$, for any Γ_1.

B. Differential Equation w.r.t. s for $M(s,a)$

Based on (17) and (30) we can write

$$M(s,a) = \frac{1}{(1-s)^N} {}_1F_1\left(N; N_{\mathrm{R}}; \frac{as}{1-s}\right). \tag{31}$$

In Appendix A, manipulation and differentiation w.r.t. s of (31) followed by substitution into the differential equation for ${}_1F_1(N; N_{\mathrm{R}}; \sigma)$ from (27) have yielded the following differential equation w.r.t. s for $M(s,a)$, in (67):

$$\begin{aligned} \big(s(1-s)^2\partial_s^2 - [2(N+1)s(1-s) - (1-s)N_{\mathrm{R}} + as]\partial_s \\ + N[(N+1)s - N_{\mathrm{R}} - a]\big) M(s,a) = 0. \end{aligned} \tag{32}$$

Because s^l appears in front of ∂_s^k in (32), the corresponding differential equation for $p(t,a)$ cannot be obtained by inverse-Laplace transform. Therefore, we shall first employ the following order-changing rule, which can readily be deduced from [36, Th. 6.1.2 (Leibniz Formula), p. 282] [40, Th. 1.1.1, p. 3].

Proposition 1:

$$s^l \partial_s^k = \sum_{m=0}^{\min(l,k)} \frac{(-1)^m (l-m+1)_m (k-m+1)_m}{m!} \partial_s^{k-m} s^{l-m}.$$

From the above general rule we obtain the following particular rules

$$\begin{aligned} s\partial_s &= \partial_s s - 1, && (33)\\ s\partial_s^2 &= \partial_s^2 s - 2\partial_s, && (34)\\ s^2\partial_s &= \partial_s s^2 - 2s, && (35)\\ s^2\partial_s^2 &= \partial_s^2 s^2 - 4\partial_s s + 2, && (36)\\ s^3\partial_s^2 &= \partial_s^2 s^3 - 6\partial_s s^2 + 6s, && (37) \end{aligned}$$

which, when applied in (32), yield for $M(s,a)$ the following differential equation w.r.t. s:

$$\begin{aligned} &[\partial_s^2 s^3 - 2\partial_s^2 s^2 + \partial_s^2 s + (2N-4)\partial_s s^2 \\ &\quad + (6 - 2N - N_{\mathrm{R}} - a)\,\partial_s s + (N_{\mathrm{R}} - 2)\partial_s \\ &\quad + (N-1)(N-2)s \\ &\quad + (N-1)(2 - N_{\mathrm{R}} - a)]M(s,a) = 0. \end{aligned} \tag{38}$$

Unlike Eq. (32), Eq. (38) can be employed based on the Laplace transform to deduce the differential equation w.r.t. t for $p(t,a)$, as shown next.

C. Differential Equation w.r.t. t for $p(t,a)$

The following proposition helps transform an expression whereby the operator ∂_s^k is applied to the product $s^l M(s,a)$ into a differential equation for $p(t,a)$ w.r.t. t. Hereafter, $p^{(l)}(t,a)$ stands for the lth derivative w.r.t. t of $p(t,a)$.

Proposition 2: The integral $\int_0^\infty e^{st}\left[t^k p^{(l)}(t,a)\right]\mathrm{d}t$, which represents the Laplace transform of $t^k p^{(l)}(t,a)$ for argument $-s$, is given by:

$$\begin{cases} (-1)^l \partial_s^k [s^l M(s,a)] \\ \quad + \sum_{m=k+1}^{l} (-1)^m\, p^{(l-m)}(0+,a) \\ \quad\quad \times \frac{(m-1)!}{(m-k-1)!} s^{m-k-1}, & l \geq 1, \\ \partial_s^k M(s,a), & l = 0. \end{cases} \tag{39}$$

Proof: Follows from the well-known Laplace-transform property for higher-order derivatives from [27, Eq. (1.14.29), p. 28] and the sign change from (14).

Applying (39) for the terms in (38) yields the following Laplace-transform pairs:

$$\begin{aligned} &\partial_s^2 s^3 M(s,a) + 2!\,p(0+,a) \leftrightarrow \\ &\qquad -t^2 p^{(3)}(t,a) \\ &-2\partial_s^2 s^2 M(s,a) \leftrightarrow \\ &\qquad -2t^2 p^{(2)}(t,a) \\ &\partial_s^2 s M(s,a) \leftrightarrow \\ &\qquad -t^2 p^{(1)}(t,a) \\ &(2N-4)\partial_s s^2 M(s,a) + (2N-4)\,p(0+,a) \leftrightarrow \\ &\qquad (2N-4)\,t\,p^{(2)}(t,a) \\ &(6-2N-N_{\mathrm{R}}-a)\,\partial_s s M(s,a) \leftrightarrow \\ &\qquad -(6-2N-N_{\mathrm{R}}-a)\,t\,p^{(1)}(t,a) \\ &(N_{\mathrm{R}}-2)\partial_s M(s,a) \leftrightarrow \\ &\qquad (N_{\mathrm{R}}-2)\,t\,p(t,a) \\ &(N-1)(N-2)sM(s,a) + (N-1)(N-2)p(0+,a) \leftrightarrow \\ &\qquad -(N-1)\,(N-2)\,p^{(1)}(t,a) \\ &(N-1)(2-N_{\mathrm{R}}-a)M(s,a) \leftrightarrow \\ &\qquad (N-1)(2-N_{\mathrm{R}}-a)\,p(t,a). \end{aligned}$$

Summing the left-hand-side terms (i.e., the s-domain terms) of the above transform pairs and accounting for (38) yields the constant $N(N-1)p(0+,a)$.

Appendix B derives $p_{\gamma_1}(0+,a)$ in (69), which, along with (30), yields

$$p(0+,a) = \begin{cases} {}_1F_1(N;N_{\mathrm{R}};-a), & N=1, \\ 0, & N>1, \end{cases} \tag{40}$$

so that

$$N(N-1)p(0+,a) = 0, \quad \forall N \geq 1, \tag{41}$$

i.e., the left-hand-side terms (i.e., the t-domain terms) above sum to 0.

Then, by the uniqueness of the Laplace transform, the right-hand-side terms (i.e., the t-domain terms) of the above transform pairs also sum to 0, i.e.,

$$\begin{aligned} &-t^2 p^{(3)}(t,a) - 2t^2 p^{(2)}(t,a) - t^2 p^{(1)}(t,a) \\ &\quad +(2N-4)tp^{(2)}(t,a) - (6-2N-N_{\mathrm{R}}-a)t\,p^{(1)}(t,a) \\ &\quad +(N_{\mathrm{R}}-2)t\,p(t,a) - (N-1)(N-2)p^{(1)}(t,a) \\ &\quad +(N-1)(2-N_{\mathrm{R}}-a)\,p(t,a) = 0, \end{aligned} \tag{42}$$

which can be rewritten as follows:

$$\begin{aligned} p^{(3)}(t,a) &= \frac{(N_{\mathrm{R}}-2)t+(N-1)(2-N_{\mathrm{R}}-a)}{t^2}p(t,a) \\ &-\frac{t^2+(6-2N-N_{\mathrm{R}}-a)t+(N-1)(N-2)}{t^2}p^{(1)}(t,a) \\ &-\frac{2t^2-(2N-4)t}{t^2}p^{(2)}(t,a). \end{aligned} \tag{43}$$

Finally, by defining the function vector

$$\mathbf{p}(t,a) = \begin{pmatrix} p(t,a) & p^{(1)}(t,a) & p^{(2)}(t,a) \end{pmatrix}^{\mathcal{T}}, \tag{44}$$

we can recast (43) as the system of differential equations w.r.t. t

$$\partial_t \mathbf{p}(t,a) = \mathbf{P}(t,a)\,\mathbf{p}(t,a), \tag{45}$$

where the elements of the 3×3 companion matrix $\mathbf{P}(t,a)$ are:

$$\begin{aligned} [\mathbf{P}(t,a)]_{1,1} &= [\mathbf{P}(t,a)]_{1,3} = 0, \\ [\mathbf{P}(t,a)]_{2,1} &= [\mathbf{P}(t,a)]_{2,2} = 0, \\ [\mathbf{P}(t,a)]_{1,2} &= [\mathbf{P}(t,a)]_{2,3} = 1, \\ [\mathbf{P}(t,a)]_{3,1} &= \frac{(N_{\mathrm{R}}-2)t+(N-1)(2-N_{\mathrm{R}}-a)}{t^2}, \\ [\mathbf{P}(t,a)]_{3,2} &= -\frac{t^2+(6-2N-N_{\mathrm{R}}-a)t}{t^2}, \\ &\quad -\frac{(N-1)(N-2)}{t^2}, \\ [\mathbf{P}(t,a)]_{3,3} &= -\frac{2t^2-(2N-4)t}{t^2}. \end{aligned}$$

Note that we did not derive the above differential equations w.r.t. t in order to solve the original problem, i.e., to compute the SNR p.d.f., given K, i.e., a, over a relevant range of t, as in Fig. 1, by applying the HGM w.r.t. t based on (45). This approach would require $p(t_0,a)$ as well as its first two derivatives w.r.t. t, i.e., $p^{(1)}(t_0,a)$, and $p^{(2)}(t_0,a)$ at the given a. Appendix C derives infinite series for them. However, their computation is reliable only for a sufficiently small (i.e., practically-irrelevant K value), for the same reasons as those already discussed in Section III-D for $p_{\gamma_1}(t,a)$.

Instead, we derived the above differential equations w.r.t. t for $p(t,a)$ because its derivatives w.r.t. t from (45) shall be found to enter the differential equation for $p(t,a)$ w.r.t. a, which may be used for HGM-based computation of $\mathbf{p}(t,a)$ at relevant values of a. Therefore, next, we deduce the differential equation w.r.t. a for $p(t,a)$, which was shown to exist in Lemma 1.

D. Differential Equation w.r.t. a for $p(t,a)$

In Appendix D, Eq. (80), we have deduced the relationship

$$a\partial_a M(s,a) = \left(s\partial_s - s^2\partial_s - Ns\right) M(s,a), \tag{46}$$

which, by using the order-changing rules (33) and (35), becomes

$$\begin{aligned} a\partial_a M(s,a) &= \left(\partial_s s - 1 - \partial_s s^2 + 2s - Ns\right) M(s,a) \\ &= \left[-1 + (-Ns + \partial_s s + 2s) - \partial_s s^2\right] M(s,a). \end{aligned}$$

Transformation of the above to the t-domain based on (39) and further manipulation yield

$$\begin{aligned} a\partial_a p(t,a) &= \overbrace{(N-1)\,p(0+,a)}^{=0,\forall N} \\ &\quad -p(t,a) + (N-t-2)\,p^{(1)}(t,a) - t\,p^{(2)}(t,a) \\ &= -p(t,a) + (N-t-2)\,p^{(1)}(t,a) \\ &\quad -t\,p^{(2)}(t,a), \end{aligned} \tag{47}$$

which entwines the derivatives of $p(t,a)$ w.r.t. a and w.r.t. t; recall that the derivatives of $p(t,a)$ w.r.t. t satisfy (43).

Now, twice differentiating (47) w.r.t. t and substituting $p^{(3)}(t,a)$ from (43) yields:

$$\begin{aligned} &a\partial_a p^{(1)}(t,a) \\ &= -t\,p^{(3)}(t,a) + (N-t-3)\,p^{(2)}(t,a) - 2p^{(1)}(t,a) \\ &= \left(2 - N_{\mathrm{R}} + \frac{2-2N-N_{\mathrm{R}}-a+NN_{\mathrm{R}}+Na}{t}\right)p(t,a) \\ &\quad + \left(4 - 2N - N_{\mathrm{R}} - a + t + \frac{2+N^2-3N}{t}\right)p^{(1)}(t,a) \\ &\quad + (1-N+t)\,p^{(2)}(t,a), \end{aligned} \tag{48}$$

$$\begin{aligned} &a\partial_a p^{(2)}(t,a) \\ &= \Bigg(-2 + N_{\mathrm{R}} + \frac{-4+4N+2N_{\mathrm{R}}+a-2NN_{\mathrm{R}}-Na}{t} \\ &\qquad + \frac{-4+6N+2N_{\mathrm{R}}+2a-3NN_{\mathrm{R}}-3Na}{t^2} \\ &\qquad + \frac{N^2N_{\mathrm{R}}+N^2a-2N^2}{t^2}\Bigg)p(t,a) \\ &\quad + \Bigg(3N - 4 + a - t + \frac{-6-3N^2+9N}{t} \\ &\qquad + \frac{-4+8N-5N^2+N^3}{t^2}\Bigg)p^{(1)}(t,a) \\ &\quad + \Bigg(-1 + 2N - N_{\mathrm{R}} - a - t \\ &\qquad + \frac{-2-N^2+3N}{t}\Bigg)p^{(2)}(t,a). \end{aligned} \tag{49}$$

Finally, collecting (47)–(49) yields for the function vector $\mathbf{p}(t,a)$ defined in (44) the system of differential equations w.r.t. a

$$\partial_a \mathbf{p}(t,a) = \frac{1}{a}\,\mathbf{Q}(t,a)\,\mathbf{p}(t,a), \tag{50}$$

where the elements of 3×3 matrix $\mathbf{Q}(t,a)$ are as follows:

$$\begin{aligned}
[\mathbf{Q}(t,a)]_{1,1} &= -1,\\
[\mathbf{Q}(t,a)]_{1,2} &= N-t-2,\\
[\mathbf{Q}(t,a)]_{1,3} &= -t,\\
[\mathbf{Q}(t,a)]_{2,1} &= 2-N_{\mathrm{R}}+\frac{2-2N-N_{\mathrm{R}}-a+NN_{\mathrm{R}}+Na}{t},\\
[\mathbf{Q}(t,a)]_{2,2} &= 4-2N-N_{\mathrm{R}}-a+t+\frac{2+N^2-3N}{t},\\
[\mathbf{Q}(t,a)]_{2,3} &= 1-N+t,\\
[\mathbf{Q}(t,a)]_{3,1} &= -2+N_{\mathrm{R}}+\frac{-4+4N+2N_{\mathrm{R}}}{t}\\
&\quad+\frac{a-2NN_{\mathrm{R}}-Na}{t}\\
&\quad+\frac{-4+6N+2N_{\mathrm{R}}+2a-3NN_{\mathrm{R}}-3Na}{t^2}\\
&\quad+\frac{N^2N_{\mathrm{R}}+N^2a-2N^2}{t^2},\\
[\mathbf{Q}(t,a)]_{3,2} &= 3N-4+a-t+\frac{-6-3N^2+9N}{t}\\
&\quad+\frac{-4+8N-5N^2+N^3}{t^2},\\
[\mathbf{Q}(t,a)]_{3,3} &= -1+2N-N_{\mathrm{R}}-a-t+\frac{-2-N^2+3N}{t}.
\end{aligned}$$

E. Computation of $p(t,a)$ vs. a by HGM w.r.t. a, Given t

One may now attempt to apply HGM to solve numerically the system of differential equations (50), between some small[6] $a_0 \neq 0$ and the desired a, given t and initial condition vector $\mathbf{p}(t,a_0) = \big(p(t,a_0)\; p^{(1)}(t,a_0)\; p^{(2)}(t,a_0)\big)^{\mathcal{T}}$. The latter may be computed by truncating the infinite-series expressions derived in Appendix C.

However, we have found that, for small a_0 and large t, such computation of $p(t,a_0)$ suffers from error caused by numerical representation accuracy limitations: because $p(t,a_0)$ is then extremely small, it cannot be represented accurately; this initial-condition inaccuracy prevents HGM w.r.t. a from accurately computing $p(t,a)$ between a_0 and a.

We can avoid the numerical issues caused by computing the infinite series at large values of either a or t, by applying the HGM simultaneously w.r.t. a and t, as shown next.

F. Computation of $p(t,a)$ by HGM w.r.t. t, for $a = c\,t$

In the systems of differential equations obtained in (45) and (50), i.e., in

$$\partial_t \mathbf{p}(t,a) = \mathbf{P}(t,a)\,\mathbf{p}(t,a), \tag{51}$$

$$\partial_a \mathbf{p}(t,a) = \frac{1}{a}\,\mathbf{Q}(t,a)\,\mathbf{p}(t,a), \tag{52}$$

[6]HGM requires $a_0 \neq 0$ because a divides matrix $\mathbf{Q}$ in (50).

we now make the following changes of variables

$$t = c_1 u, \tag{53}$$

$$a = c_2 u. \tag{54}$$

Then, the bivariate function vector from (44) becomes the univariate function vector

$$\mathbf{p}(c_1u,c_2u) = \begin{pmatrix} p(c_1u,c_2u)\\ p^{(1)}(c_1u,c_2u)\\ p^{(2)}(c_1u,c_2u)\end{pmatrix} = \widetilde{\mathbf{p}}(u). \tag{55}$$

Based on the chain rule [27, Eq. (1.5.7), p. 7] as well as on (51) and (52), we can write:

$$\begin{aligned}
\frac{d}{du}\widetilde{\mathbf{p}}(u) &= \frac{d}{du}\mathbf{p}(\underbrace{c_1u}_{t},\underbrace{c_2u}_{a})\\
&= \left[\partial_t\mathbf{p}(t,a)\frac{dt}{du}+\partial_a\mathbf{p}(t,a)\frac{da}{du}\right]\Bigg|_{\substack{t=c_1u\\ a=c_2u}}\\
&= c_1\,\mathbf{P}(c_1u,c_2u)\,\widetilde{\mathbf{p}}(u)+c_2\,\frac{1}{c_2u}\,\mathbf{Q}(c_1u,c_2u)\,\widetilde{\mathbf{p}}(u)\\
&= c_1\,\mathbf{P}(c_1u,c_2u)\,\widetilde{\mathbf{p}}(u)+\frac{1}{u}\,\mathbf{Q}(c_1u,c_2u)\,\widetilde{\mathbf{p}}(u).
\end{aligned} \tag{56}$$

Then, for example, $c_1 = 1$ and $c_2 = c$, i.e., $a = c\,t$, yields the system of differential equations

$$\frac{d}{du}\widetilde{\mathbf{p}}(u) = \left[\mathbf{P}(u,c\,u)+\frac{1}{u}\,\mathbf{Q}(u,c\,u)\right]\widetilde{\mathbf{p}}(u), \tag{57}$$

which helps apply HGM for $a = c\,t$, i.e., simultaneously w.r.t. a and t.

Finally, note that from $p(t,a)$ computed with the HGM as above we can recover the SNR p.d.f. $p_{\gamma_1}(t,a)$ with (30). Then, numerical integration of $p_{\gamma_1}(t,a)$ yields the outage probability and ergodic capacity based on (21) and (22), respectively. Relevant results are shown next.

VI. Numerical Results

A. Settings and Approach

The numerical results presented below have been obtained for a MIMO system with $N_{\mathrm{R}} = 6$ and $N_{\mathrm{T}} = 2$ under Rician–Rayleigh fading with $K = 7$ dB and AS $= 51°$, i.e., the means of their WINNER II lognormal distributions for the indoor scenario A1 [9], as follows:

- Monte-Carlo simulation: random samples of the channel matrix $\mathbf{H}$ have been generated based on the model (5); the ZF SNR for Stream 1 has been computed for each sample by using (12); a histogram of the samples has yielded the p.d.f. and c.d.f..
- Analysis: from expressions (24), (25) and (26) and from HGM for differential equation (57). When necessary, we have integrated numerically using the rectangle method.

We now outline our HGM-based procedure based on (57) for the computation of the ZF SNR p.d.f. and ensuing performance measures. Given Γ_{s} defined in (3) and the Rician K-factor, we have computed Γ_1 and a with (15) and (16), respectively. Then, we have computed the Stream-1 ZF SNR p.d.f. over the SNR range with the following steps:

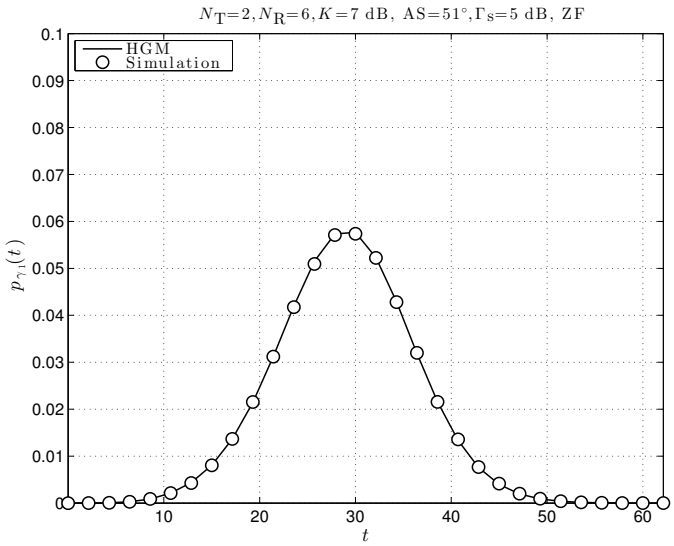

Fig. 2. Stream-1 SNR p.d.f. computed by the HGM, based on (57), and by Monte-Carlo simulation, for $N_{\rm R} = 6$, $N_{\rm T} = 2$, and Rician–Rayleigh fading with $K = 7$ dB, AS $= 51°$.

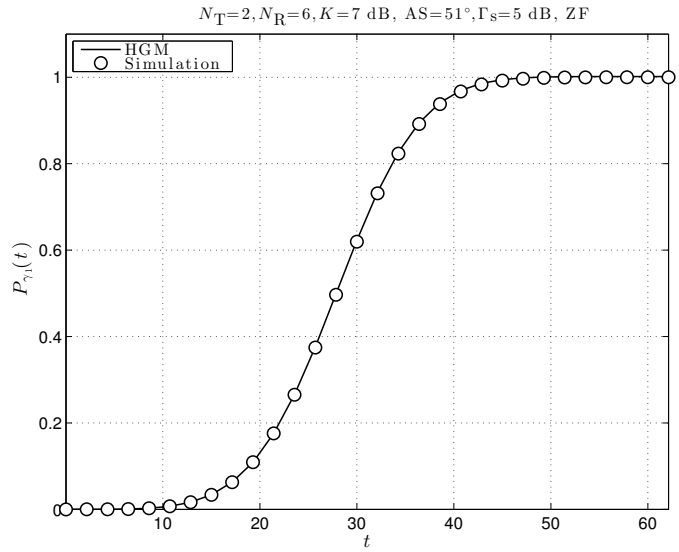

Fig. 3. Stream-1 SNR c.d.f. computed by numerical integration of the p.d.f. output by the HGM, based on (57), and by Monte-Carlo simulation, for $N_{\rm R} = 6$, $N_{\rm T} = 2$, and Rician–Rayleigh fading with $K = 7$ dB, AS $= 51°$.

1) Compute accurately the initial condition[7] $\widetilde{\mathbf{p}}(u_0) = \big(p(u_0, u_0)\; p^{(1)}(u_0, u_0)\; p^{(2)}(u_0, u_0)\big)^{\mathcal{T}}$ for a sufficiently-small u_0, using the infinite series for $p^{(q)}(t, a)$ derived in Appendix C.
2) Sample the SNR range of interest $[u_1, u_M]$ as $u_1, u_2, \cdots, u_M$.
3) For each sample $u = u_m$, $m = 1, 2, \cdots, M$, set $c = a/u$, use HGM to solve (57) from u_0 to u, and save the final value $p(u, cu)$, which represents $p(t, a)$ on the line $a = c\,t$.
4) Recover the ZF SNR p.d.f. based on (30), i.e., with $p_{\gamma_1}(t, a) = p(t/\Gamma_1, a)/\Gamma_1$.

This approach avoids using the infinite series for $p(t, a)$, $p^{(1)}(t, a)$, and $p^{(2)}(t, a)$ for either large a or large t, and, thus, avoids the ensuing numerical issues described in Sections III-D and V-E.

Finally, we have integrated numerically the p.d.f. output by the HGM, according to (21) and (22), to compute the outage probability and ergodic capacity, respectively.

B. Description of Results

Figs. 2 and 3 depict, respectively, the SNR p.d.f. and c.d.f. computed with the HGM as above, and by simulation. The HGM is successful, i.e., the resulting p.d.f. and c.d.f. agree with the simulation, and the c.d.f. shown in Fig 3 (from numerically integrating the p.d.f. output by the HGM) goes to 1 for increasing t. Recall that in [7] [8] we had been able to accurately compute $p_{\gamma_1}(t)$ based on its infinite series (20) only up to the unrealistically-small K value of 1.5 dB. This has also been illustrated herein in Fig. 1, where the series-based computation breaks down for $K = 7$ dB. Consequently, Figs. 2 and 3 do not attempt to plot series results.

[7]Note that both t and a are substituted with u_0 in this step.

Finally, Figs. 4 and 5 depict, respectively, the outage probability and ergodic capacity (in bpcu) with respect to $\Gamma_{\rm b}$ defined in (4). For Rayleigh-only fading we have used the integral expressions (25) and (26), respectively. For Rician–Rayleigh fading we have integrated numerically according to (21) and (22), respectively, the SNR p.d.f. computed with the HGM as shown above. The HGM and simulation results agree closely[8]. On the other hand, results from $P_{\rm o}$ and C infinite series [7, Eqs. (69), (71)] could not be shown because their computation breaks down.

C. HGM Complexity

Our HGM-based computation solves (57) with the iterative Runge–Kutta method [27, Section 3.7] [37], for tolerance level $\epsilon = 10^{-15}$ (i.e., 15 digits of accuracy), with the `MATLAB` `ode` function. Implementations of the Runge-Kutta method are available in most numerical tools, and their complexity is known to be polynomial in the number of digits of accuracy [41, p. 33] [42] [43]. In our numerical experiments we have found that the duration of the HGM-based computation is reasonable[9]. Finally, HGM-based computation duration and success are robust to the value of K, unlike infinite-series-based computation [7] [8] [29].

[8]Unshown results have revealed that HGM yields accurate results even for K as high as 15 dB, and also for other combinations of $N_{\rm T}$ and $N_{\rm R}$, without a noticeable increase in computation time.

[9]Computation of the p.d.f. at 30 samples of t, as shown in Fig. 2 requires about 60 seconds. Then, outage probability computation for one $\Gamma_{\rm b}$ value takes about 70 s. Finally, ergodic capacity computation for one $\Gamma_{\rm b}$ value takes about 140 s.

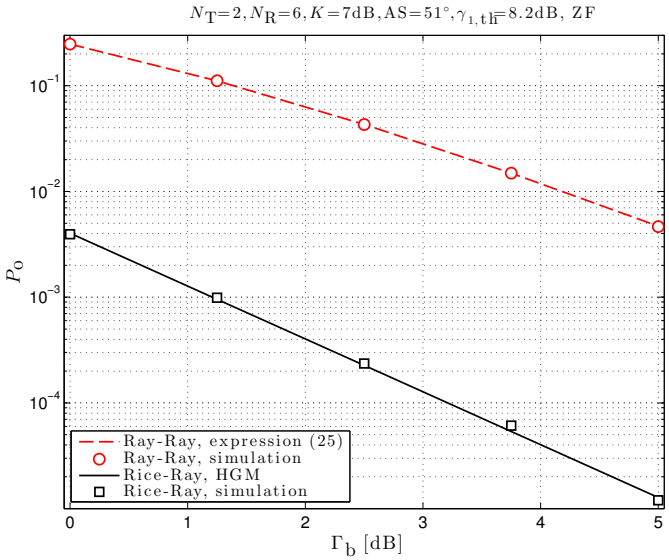

Fig. 4. Stream-1 outage probability for $N_R = 6$, $N_T = 2$, and fading parameters $K = 7$ dB, AS $= 51°$. For Rayleigh-only fading: from expression (25) and from simulation. For Rician–Rayleigh fading: from numerical integration according to (21) of the SNR p.d.f. computed with the HGM, based on (57), and from simulation.

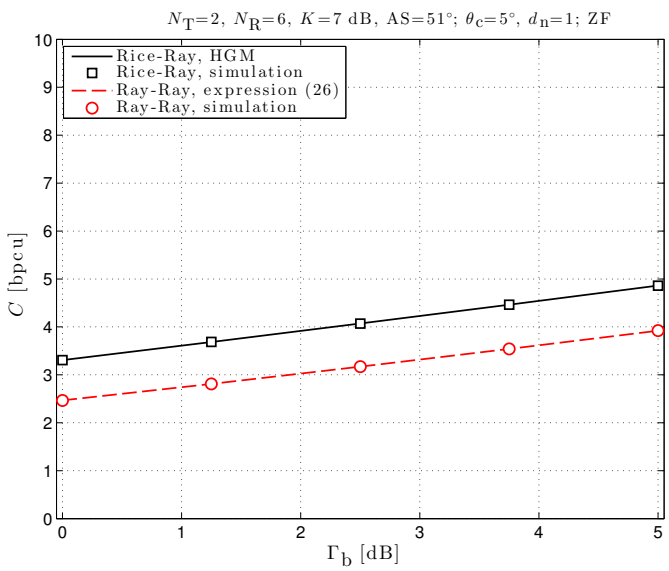

Fig. 5. Stream-1 ergodic capacity for $N_R = 6$, $N_T = 2$, and fading parameters $K = 7$ dB, AS $= 51°$. For Rayleigh-only fading: from expression (26) and from simulation. For Rician–Rayleigh fading: from numerical integration according to (22) of the SNR p.d.f. computed with the HGM, based on (57), and from simulation.

VII. Future Work: an HGM-Based Framework for MIMO Evaluation

A. HGM-Based Performance Evaluation of MIMO under General Fading

For many fading types (e.g., Rayleigh, Rician, Nakagami, lognormal) and for many multiantenna transmission techniques, previous work, e.g. [2], showed expressions for the SNR m.g.f. that involve special (e.g., hypergeometric, Bessel) functions of scalar argument, which have typically been written as infinite-series, but are also holonomic. Furthermore, [32] proposed generalizing MIMO analysis by purposely writing as infinite series (ensuing from expansions around 0) the SNR m.g.f. for several widely-used fading types. We have applied a similar approach in [44] for $N_R \times 2$ MIMO ZF under full-Rician fading. However, the deduced SNR p.d.f. expression is a mixture of finite and infinite series whose computation by truncation has been found accurate only for unrealistically-small K values. Then, one may attempt to apply instead the HGM-based approach: deduce and solve the relevant differential equations.

Further, hypergeometric functions also of matrix argument have often occurred in MIMO analyses due to statistical assumptions about the channel matrix [30] [31]. For example, the c.d.f. and m.g.f. of the dominant eigenvalue of a complex-valued central-Wishart-distributed matrix have been expressed in terms of ${}_1F_1(a;c;\mathbf{R})$ and ${}_2F_1(a;c;\mathbf{R})$ in [31, Eqs. (34), (42)], respectively. Thus, for MIMO beamforming under Rayleigh-fading channel, the average error probability and outage probability have been expressed in terms of ${}_1F_1(a;c;\mathbf{R})$ and ${}_2F_1(a;c;\mathbf{R})$ in [31, Eqs. (30), (22)], respectively. Unfortunately, the well-known infinite series for these functions (and the zonal polynomials involved) [45, Eq. (1.1)] [30, Eq. (1.1)] [31, Eq. (61)] are difficult to compute [30] [31]. Nevertheless, such functions also satisfy differential equations [45] [46]. Those for ${}_1F_1(a;c;\mathbf{R})$ from [45, Eq. (5.1)] have recently been exploited for the accurate HGM-based computation of the c.d.f. of the dominant eigenvalue of a real-valued central-Wishart-distributed matrix in [38]. We shall extend this approach to complex-valued matrices, in order to evaluate MIMO beamforming performance.

B. Automated Deduction of Differential Equations

In the current paper, HGM has been applied for solving differential equations for the ZF SNR m.g.f. and p.d.f. that we deduced manually. Software tools that can help automate the deduction of differential equations for holonomic functions have recently become available [35, p. 171] [36, Ch. 7] [47] [48]. Thus, in other current work [49], we investigate employing and enhancing such tools to automatically derive differential equations not only for the SNR m.g.f. and p.d.f., but also for the outage probability and ergodic capacity.

Finally, we shall investigate whether such automated tools can help make HGM applicable to MIMO performance evaluation under a wide range of fading types, by deducing differential equations — instead of infinite series, as in [2] [44] [32]. The outcome of this future work is envisioned to be a framework for the automated analysis and HGM-based evaluation of MIMO transceiver performance under general fading.

VIII. Summary and Conclusions

For MIMO ZF under Rician–Rayleigh fading, this paper has demonstrated that performance-measure expressions can be evaluated accurately, by using the HGM, at (realistic) Rician K-factor values that render unusable the conventional method of truncating infinite series. For the SNR m.g.f., which has

been known in terms of the confluent hypergeometric function, which is a holonomic function, we have deduced the satisfied differential equations. They have yielded the differential equations satisfied by the SNR p.d.f., which, in turn, have helped compute the p.d.f. accurately using the HGM at values of K relevant according to WINNER II (e.g., $K = 7$ dB). Finally, numerical integration of the SNR p.d.f. obtained by the HGM has yielded for the MIMO ZF outage probability and ergodic capacity close agreement with simulations.

Future work shall attempt to extend the results of this paper into an automated HGM-based analysis and evaluation framework that promises to accurately characterize MIMO performance for realistic fading-parameter values.

Appendix A
Differential Equation w.r.t. s for $M(s,a)$

First, substituting σ with $\frac{as}{1-s}$ in the differential equation for ${}_1F_1(N;N_{\mathrm{R}};\sigma)$ from (27) yields

$$\begin{aligned}&\frac{as}{1-s}{}_1F_1^{(2)}\left(N;N_{\mathrm{R}};\frac{as}{1-s}\right)\\&+\left(N_{\mathrm{R}}-\frac{as}{1-s}\right){}_1F_1^{(1)}\left(N;N_{\mathrm{R}};\frac{as}{1-s}\right)\\&-N{}_1F_1\left(N;N_{\mathrm{R}};\frac{as}{1-s}\right)=0.\end{aligned}\tag{58}$$

Then, from (31), we have

$$M(s,a)=\frac{1}{(1-s)^N}{}_1F_1\left(N;N_{\mathrm{R}};\frac{as}{1-s}\right),\tag{59}$$

which yields

$${}_1F_1\left(N;N_{\mathrm{R}};\frac{as}{1-s}\right)=(1-s)^N M(s,a).\tag{60}$$

Differentiating (59) w.r.t. s yields:

$$\begin{aligned}\partial_s M(s,a) &= \frac{N}{(1-s)^{N+1}}{}_1F_1\left(N;N_{\mathrm{R}};\frac{as}{1-s}\right)\\&\quad+\frac{a}{(1-s)^{N+2}}{}_1F_1^{(1)}\left(N;N_{\mathrm{R}};\frac{as}{1-s}\right)\end{aligned}\tag{61}$$

By first substituting (60) into (61) and then by differentiating the result w.r.t. s we obtain

$$\begin{aligned}\partial_s M(s,a) &= \frac{N}{(1-s)}M(s,a)\\&\quad+\frac{a}{(1-s)^{N+2}}{}_1F_1^{(1)}\left(N;N_{\mathrm{R}};\frac{as}{1-s}\right)\end{aligned}\tag{62}$$

$$\begin{aligned}\partial_s^2 M(s,a) &= \frac{N}{(1-s)^2}M(s,a)+\frac{N}{(1-s)}\partial_s M(s,a)\\&\quad+\frac{a(N+2)}{(1-s)^{N+3}}{}_1F_1^{(1)}\left(N;N_{\mathrm{R}};\frac{as}{1-s}\right)\\&\quad+\frac{a^2}{(1-s)^{N+4}}{}_1F_1^{(2)}\left(N;N_{\mathrm{R}};\frac{as}{1-s}\right)\end{aligned}\tag{63}$$

which yield, respectively:

$$\begin{aligned}&{}_1F_1^{(1)}\left(N;N_{\mathrm{R}};\frac{as}{1-s}\right)\\&=\frac{(1-s)^{N+2}}{a}\left[\partial_s-\frac{N}{(1-s)}\right]M(s,a),\end{aligned}\tag{64}$$

$$\begin{aligned}&{}_1F_1^{(2)}\left(N;N_{\mathrm{R}};\frac{as}{1-s}\right)\\&=\frac{(1-s)^{N+4}}{a^2}\Bigg[\partial_s^2M(s,a)-\frac{N}{(1-s)^2}M(s,a)\\&\quad-\frac{N}{(1-s)}\partial_s M(s,a)\\&\quad-\frac{a(N+2)}{(1-s)^{N+3}}{}_1F_1^{(1)}\left(N;N_{\mathrm{R}};\frac{as}{1-s}\right)\Bigg].\end{aligned}\tag{65}$$

Substituting (64) into (65) yields:

$$\begin{aligned}{}_1F_1^{(2)}\left(N;N_{\mathrm{R}};\frac{as}{1-s}\right) &= \frac{(1-s)^{N+4}}{a^2}\Bigg[\partial_s^2-\frac{2(N+1)}{(1-s)}\partial_s\\&\quad+\frac{N(N+1)}{(1-s)^2}\Bigg]M(s,a).\end{aligned}\tag{66}$$

Finally, substituting (60), (64), and (66) into the differential equation (58), and further manipulation, yield the following differential equation w.r.t. s for $M(s,a)$

$$\begin{aligned}&\Big(s(1-s)^2\partial_s^2-\big[2(N+1)s(1-s)-(1-s)N_{\mathrm{R}}+as\big]\partial_s\\&\quad+N\big[(N+1)s-N_{\mathrm{R}}-a\big]\Big)M(s,a)=0,\end{aligned}\tag{67}$$

which appears in the main text in (32).

Appendix B
Initial Condition $p_{\gamma_1}(0+,a)$

For the special case with $N=1$, i.e., for $N_{\mathrm{R}}=N_{\mathrm{T}}$, (20) becomes

$$p_{\gamma_1}(t,a)=\frac{e^{-t/\Gamma_1}}{\Gamma_1}\sum_{n=0}^{\infty}A_n(a)\sum_{m=0}^{n}\binom{n}{m}\frac{(-1)^m t^{n-m}}{(n-m)!\,\Gamma_1^{n-m}},$$

which yields

$$\begin{aligned}\lim_{t\to0,t>0}p_{\gamma_1}(t,a) &= p_{\gamma_1}(0+,a)=\frac{1}{\Gamma_1}\sum_{n=0}^{\infty}A_n(a)(-1)^n\\&=\frac{1}{\Gamma_1}\sum_{n=0}^{\infty}\frac{(N)_n}{(N_{\mathrm{R}})_n}\frac{(-a)^n}{n!}.\end{aligned}\tag{68}$$

Thus, (68), (18), and (20) yield

$$p_{\gamma_1}(0+,a)=\begin{cases}\frac{1}{\Gamma_1}{}_1F_1(N;N_{\mathrm{R}};-a), & N=1\\0, & N>1,\end{cases}\tag{69}$$

which is used in the main text to deduce (40), on page 7.

APPENDIX C
INFINITE-SERIES EXPRESSIONS OF DERIVATIVES OF $p(t,a)$ W.R.T. t

Based on (20) and (30), let us define the function

$$f(t,a) = p(t,a)e^t = \sum_{n=0}^{\infty} A_n(a) \sum_{m=0}^{n} \binom{n}{m} \times \frac{(-1)^m t^{N+n-m-1}}{(N+n-m-1)!}, \quad (70)$$

whose first two derivatives are given by

$$f^{(1)}(t,a) = p^{(1)}(t,a)e^t + p(t,a)e^t,$$
$$f^{(2)}(t,a) = p^{(2)}(t,a)e^t + 2p^{(1)}(t,a)e^t + p(t,a)e^t.$$

The above yield

$$p(t,a) = f(t,a)e^{-t}, \quad (71)$$

as well as

$$p^{(1)}(t,a) = \left[f^{(1)}(t,a) - f(t,a)\right] e^{-t}, \quad (72)$$
$$p^{(2)}(t,a) = \left[f^{(2)}(t,a) - 2f^{(1)}(t,a) + f(t,a)\right] e^{-t} \quad (73)$$

which are the only derivatives of $p(t,a)$ required for (44).

Now, if we rewrite $f(t,a)$ from (70) further as

$$f(t,a) = t^{N-1} \underbrace{\sum_{n=0}^{\infty} A_n(a) \sum_{m=0}^{n} \binom{n}{m} \frac{(-1)^m t^{n-m}}{(N-1+n-m)!}}_{g(t,a)} = t^{N-1} g(t,a), \quad (74)$$

then its qth partial derivative w.r.t. t is[10], based on Leibniz's formula [27, Eq. (1.4.12), p. 5]:

$$f^{(q)}(t,a) = \partial_t^q \left[t^{N-1} g(t,a)\right] = \sum_{k=0}^{q} \binom{q}{k} \left[t^{N-1}\right]^{(k)} g^{(q-k)}(t,a) \quad (75)$$
$$= \sum_{k=0}^{q} \binom{q}{k} \frac{(N-1)! t^{N-1-k} g^{(q-k)}(t,a)}{(N-1-k)!} \quad (76)$$

If we rewrite $g(t,a)$ from (74) as

$$g(t,a) = \sum_{n=0}^{\infty} A_n(a) \sum_{r=0}^{n} \binom{n}{n-r} \frac{(-1)^{n-r} t^r}{(N-1+r)!},$$

then its partial derivative of order $q \geq 1$ w.r.t. t is given by

$$g^{(q)}(t,a) = \sum_{n=q}^{\infty} A_n(a) \sum_{r=q}^{n} \binom{n}{n-r} \times \frac{(-1)^{n-r}}{(N-1+r)!} \frac{r!}{(r-q)!} t^{r-q}, \quad (77)$$

which, along with (76), yields $f^{(q)}(t,a)$. Finally, substituting into (72) and (73) yields expressions for $p^{(1)}(t,a)$ and $p^{(2)}(t,a)$, respectively.

However, because (76) follows from (75) only for $k \leq N-1$, and because k goes from 0 to q, it is required that $N-1 \geq q$. Then, because (44) requires $f^{(q)}(t,a)$ for q as high as 2, $f^{(q)}(t,a)$ can be written as in (76) only if $N \geq 3$. Table I characterizes the remaining cases.

[10]Note that (76) follows from (75) only for $k \leq N-1$.

TABLE I
DERIVATIVES OF $f(t,a)$ FOR $N = 1, 2$

	$N=1$	$N=2$
$f(t,a)$	$g(t,a)$	$tg(t,a)$
$f^{(1)}(t,a)$	$g^{(1)}(t,a)$	$g(t,a) + tg^{(1)}(t,a)$
$f^{(2)}(t,a)$	$g^{(2)}(t,a)$	$2g^{(1)}(t,a) + tg^{(2)}(t,a)$

APPENDIX D
RELATIONSHIP BETWEEN DERIVATIVES OF $M(s,a)$ W.R.T. s AND a

Differentiating (59) w.r.t. a yields

$$\partial_a M(s,a) = \frac{s}{(1-s)^{N+1}} {}_1F_1^{(1)}\left(N; N_{\mathrm{R}}; \frac{as}{1-s}\right), \quad (78)$$

so that

$${}_1F_1^{(1)}\left(N; N_{\mathrm{R}}; \frac{as}{1-s}\right) = \frac{(1-s)^{N+1}}{s} \partial_a M(s,a). \quad (79)$$

Now, by substituting (60) and (79) into (61), and by further manipulation, we obtain

$$a\partial_a M(s,a) = s(1-s)\partial_s M(s,a) - NsM(s,a), \quad (80)$$

which appears in the main text in (46).

ACKNOWLEDGMENTS

The first version of this paper was prepared when the first author was with the Graduate School of Information Science and Technology, University of Tokyo, supported by Japan Science and Technology Agency (also for the publication of this paper). The second (accepted) version was prepared after he joined the Graduate School of Information Science and Technology, Osaka University.

Akimichi Takemura acknowledges the support of the Japan Society for the Promotion of Science (JSPS) grant-in-aid for scientific research No. 25220001, Japan Science and Technology Agency.

Hyundong Shin acknowledges the support of the National Research Foundation of Korea (NRF) grants No. 2009-0083495 and No. 2013-R1A1A2-019963, funded by the Ministry of Science, ICT & Future Planning (MSIP).

Christoph Koutschan acknowledges the support of the Austrian Science Fund (FWF) W1214.

REFERENCES

[1] A. J. Paulraj, D. A. Gore, R. U. Nabar, and H. Bolcskei, "An overview of MIMO communications–A key to gigabit wireless," *Proc. of the IEEE*, vol. 92, no. 2, pp. 198–218, February 2004.

[2] M. K. Simon and M.-S. Alouini, *Digital Communication Over Fading Channels. A Unified Approach to Performance Analysis*. Baltimore, Maryland: John Wiley and Sons, 2000.

[3] D. Gesbert, M. Kountouris, R. W. Heath, C.-B. Chae, and T. Salzer, "Shifting the MIMO paradigm," *IEEE Signal Processing Magazine*, vol. 24, no. 5, pp. 36–46, 2007.

[4] M. McKay, A. Zanella, I. Collings, and M. Chiani, "Error probability and SINR analysis of optimum combining in Rician fading," *IEEE Transactions on Communications*, vol. 57, no. 3, pp. 676–687, March 2009.

[5] J. Hoydis, S. ten Brink, and M. Debbah, "Massive MIMO in the UL/DL of cellular networks: How many antennas do we need?" *IEEE Journal on Selected Areas in Communications*, vol. 31, no. 2, pp. 160–171, 2013.

[6] C. Siriteanu, Y. Miyanaga, S. D. Blostein, S. Kuriki, and X. Shi, "MIMO zero-forcing detection analysis for correlated and estimated Rician fading," *IEEE Transactions on Vehicular Technology*, vol. 61, no. 7, pp. 3087–3099, September 2012.

[7] C. Siriteanu, S. D. Blostein, A. Takemura, H. Shin, S. Yousefi, and S. Kuriki, "Exact MIMO zero-forcing detection analysis for transmit-correlated Rician fading," *IEEE Transactions on Wireless Communications*, vol. 13, no. 3, pp. 1514–1527, March 2014.

[8] C. Siriteanu, A. Takemura, S. D. Blostein, S. Kuriki, and H. Shin, "Convergence analysis of performance-measure expressions for MIMO ZF under Rician fading," in *Australian Communications Theory Workshop, (AUSCTW'14), Sydney, Australia*, Feb. 2014.

[9] P. Kyosti, J. Meinila, L. Hentila, and *et al.*, "WINNER II Channel Models. Part I," CEC, Tech. Rep. IST-4-027756, 2008.

[10] L. Bai and J. Choi, *Low complexity MIMO detection*. Springer, 2012.

[11] Q. Li, G. Li, W. Lee, M. Lee, D. Mazzarese, B. Clerckx, and Z. Li, "MIMO techniques in WiMAX and LTE: a feature overview," *IEEE Communications Magazine*, vol. 48, no. 5, pp. 86–92, May 2010.

[12] M. Jung, Y. Kim, J. Lee, and S. Choi, "Optimal number of users in zero-forcing based multiuser MIMO systems with large number of antennas," *Journal of Communications and Networks*, vol. 15, no. 4, pp. 362–369, 2013.

[13] M. Matthaiou, C. Zhong, M. McKay, and T. Ratnarajah, "Sum rate analysis of ZF receivers in distributed MIMO systems," *IEEE Journal on Selected Areas in Communications*, vol. 31, no. 2, pp. 180–191, 2013.

[14] H. Ngo, E. Larsson, and T. Marzetta, "The multicell multiuser MIMO uplink with very large antenna arrays and a finite-dimensional channel," *IEEE Transactions on Communications*, vol. 61, no. 6, pp. 2350–2361, 2013.

[15] D. A. Basnayaka, P. J. Smith, and P. A. Martin, "Performance analysis of macrodiversity MIMO systems with MMSE and ZF receivers in flat Rayleigh fading," *IEEE Trans. on Wireless Communications*, vol. 12, no. 5, pp. 2240–2251, 2013.

[16] H. Artes, D. Seethaler, and F. Hlawatsch, "Efficient detection algorithms for MIMO channels: a geometrical approach to approximate ML detection," *IEEE Transactions on Signal Processing*, vol. 51, no. 11, pp. 2808–2820, Nov. 2003.

[17] D. Gesbert, "Robust linear MIMO receivers: A minimum error-rate approach," *IEEE Transactions on Signal Processing*, vol. 51, no. 11, pp. 2863–2871, 2003.

[18] X. Ma and W. Zhang, "Fundamental limits of linear equalizers: diversity, capacity, and complexity," *IEEE Transactions on Information Theory*, vol. 54, no. 8, pp. 3442–3456, 2008.

[19] J. Maurer, J. Jaldén, D. Seethaler, and G. Matz, "Achieving a continuous diversity-complexity tradeoff in wireless MIMO systems via pre-equalized sphere-decoding," *IEEE Journal of Selected Topics in Signal Processing*, vol. 3, no. 6, pp. 986–999, 2009.

[20] J. H. Winters, J. Salz, and R. D. Gitlin, "The impact of antenna diversity on the capacity of wireless communication systems," *IEEE Transactions on Communications*, vol. 42, no. 234, pp. 1740–1751, 1994.

[21] R. Louie, M. McKay, and I. Collings, "New performance results for multiuser optimum combining in the presence of Rician fading," *IEEE Transactions on Communications*, vol. 57, no. 8, pp. 2348–2358, Aug. 2009.

[22] P. Li, D. Paul, R. Narasimhan, and J. Cioffi, "On the distribution of SINR for the MMSE MIMO receiver and performance analysis," *IEEE Transactions on Information Theory*, vol. 52, no. 1, pp. 271–286, 2006.

[23] Y. Jiang, M. Varanasi, and J. Li, "Performance analysis of ZF and MMSE equalizers for MIMO systems: An in-depth study of the high SNR regime," *IEEE Transactions on Information Theory*, vol. 57, no. 4, pp. 2008–2026, April 2011.

[24] A. H. Mehana and A. Nosratinia, "Diversity of MMSE MIMO receivers," *IEEE Transactions on Information Theory*, vol. 58, no. 11, pp. 6788–6805, 2012.

[25] D. A. Gore, R. W. Heath Jr, and A. J. Paulraj, "Transmit selection in spatial multiplexing systems," *IEEE Communications Letters*, vol. 6, no. 11, pp. 491–493, 2002.

[26] M. Kiessling and J. Speidel, "Analytical performance of MIMO zero-forcing receivers in correlated Rayleigh fading environments," in *IEEE Workshop on Signal Processing Advances in Wireless Communications (SPAWC'03)*, June 2003, pp. 383–387.

[27] F. W. J. Olver, D. W. Lozier, R. F. Boisvert, and C. W. Clarck, Eds., *NIST Handbook of Mathematical Functions*. Cambridge University Press, 2010.

[28] K. J. Kim, Y. Fan, R. A. Iltis, H. V. Poor, and M. H. Lee, "A reduced feedback precoder for MIMO–OFDM cooperative diversity systems," *IEEE Transactions on Vehicular Technology*, vol. 61, no. 2, pp. 584–596, Feb. 2012.

[29] K. E. Muller, "Computing the confluent hypergeometric function, $M(a, b, x)$," *Numerische Mathematik*, vol. 90, no. 1, pp. 179–196, 2001.

[30] P. Koev and A. Edelman, "The efficient evaluation of the hypergeometric function of a matrix argument," *Mathematics of Computation*, vol. 75, no. 254, pp. 833–846, 2006.

[31] A. J. Grant, "Performance analysis of transmit beamforming," *IEEE Transactions on Communications*, vol. 53, no. 4, pp. 738–744, 2005.

[32] G. A. Ropokis, A. A. Rontogiannis, P. T. Mathiopoulos, and K. Berberidis, "An exact performance analysis of MRC/OSTBC over generalized fading channels," *IEEE Transactions on Communications*, vol. 58, no. 9, pp. 2486–2492, 2010.

[33] D. Zeilberger, "A holonomic systems approach to special functions identities," *Journal of computational and applied mathematics*, vol. 32, no. 3, pp. 321–368, 1990.

[34] C. Mallinger, "Algorithmic manipulations and transformations of univariate holonomic functions and sequences," Ph.D. dissertation, Johannes Kepler University Linz, Austria, 1996.

[35] M. Kauers and P. Paule, *The Concrete Tetrahedron: Symbolic Sums, Recurrence Equations, Generating Functions, Asymptotic Estimates*. Springer Wien, 2011.

[36] T. Hibi, Ed., *Grobner Bases. Statistics and Software Systems*. Tokyo, Japan: Springer, 2013.

[37] T. Sei and A. Kume, "Calculating the normalising constant of the Bingham distribution on the sphere using the holonomic gradient method," *Statistics and Computing*, pp. 1–12, 2013.

[38] H. Hashiguchi, Y. Numata, N. Takayama, and A. Takemura, "The holonomic gradient method for the distribution function of the largest root of a Wishart matrix," *Journal of Multivariate Analysis*, vol. 117, pp. 296–312, 2013.

[39] S. Loyka and G. Levin, "On physically-based normalization of MIMO channel matrices," *IEEE Transactions on Wireless Communications*, vol. 8, no. 3, pp. 1107–1112, March 2009.

[40] M. Saito, B. Sturmfels, and N. Takayama, *Gröbner Deformations of Hypergeometric Differential Equations*, ser. Algorithms and Computation in Mathematics. Springer, 2011.

[41] S. Ilie, "Computational complexity of numerical solutions of initial value problems for differential algebraic equations," Ph.D. dissertation, The University of Western Ontario, 2005.

[42] S. Ilie, R. M. Corless, and C. Essex, "The computational complexity of extrapolation methods," *Mathematics in Computer Science*, vol. 2, no. 4, pp. 557–566, 2009.

[43] S. Ilie, G. Söderlind, and R. M. Corless, "Adaptivity and computational complexity in the numerical solution of odes," *Journal of Complexity*, vol. 24, no. 3, pp. 341–361, 2008.

[44] C. Siriteanu, A. Takemura, S. Kuriki, D. Richards, T. Onoye, and H. Shin, "Performance analysis of $N_{\mathrm{R}} \times 2$ MIMO zero-forcing for full-Rician fading," *IEEE Transactions on Wireless Communications, to be submitted*, October 2014.

[45] R. J. Muirhead, "Systems of partial differential equations for hypergeometric functions of matrix argument," *The Annals of Mathematical Statistics*, vol. 41, no. 3, pp. 991–1001, 1970.

[46] Y. Chikuse, "Partial differential equations for hypergeometric functions of complex argument matrices and their applications," *Annals of the Institute of Statistical Mathematics*, vol. 28, no. 1, pp. 187–199, 1976.

[47] C. Koutschan, "Advanced applications of the holonomic systems approach," Ph.D. dissertation, Research Institute for Symbolic Computation (RISC), Johannes Kepler University, Linz, Austria, 2009. [Online]. Available: http://www.risc.jku.at/research/combinat/software/HolonomicFunctions/

[48] ——, "HolonomicFunctions (user's guide)," RISC Report Series, Johannes Kepler University, Linz, Austria, Tech. Rep. 10-01, 2010. [Online]. Available: http://www.risc.jku.at/research/combinat/software/HolonomicFunctions/

[49] C. Siriteanu, C. Koutschan, T. Onoye, and A. Takemura, "Automated mimo performance analysis and evaluation using the holonomic gradient method," *IEEE Transactions on Wireless Communications, to be submitted*, November 2014.

Constantin (Costi) Siriteanu was born in Sibiu, Romania. He received the Bachelor and Master degrees in Control Systems from "Gheorghe Asachi" Technical University, Iasi, Romania, in 1995 and 1996, respectively, and the Ph.D. degree in Electrical and Computer Engineering from Queen's University, Canada, in 2006. His Ph.D. thesis was on the performance–complexity tradeoff for smart antennas. Between September 2006 and March 2014 he worked as Researcher and Assistant Professor in Korea (Seoul National University, Kyung Hee Univesity, Hanyang University), Canada (Queen's University), and Japan (Hokkaido University, University of Tokyo). Since April 2014, he is a CAREN Specially-Appointed Assistant Professor with the Graduate School of Information Science and Technology, Osaka University. His research interests have been in developing multivariate statistics concepts that help analyze and evaluate the performance of multiple-input/multiple-output (MIMO) wireless communications systems under realistic statistical assumptions about channel fading. Recently, Constantin has been working on applications of computer algebra to the deduction of implicit representations of MIMO performance measures (i.e., as solutions of differential equations).

Akimichi Takemura received the Bachelor of Arts degree in Economics in 1976 and the Master of Arts degree in Statistics in 1978 from University of Tokyo, and the Ph.D. degree in Statistics in 1982 from Stanford University. He was an acting Assistant Professor at the Department of Statistics, Stanford University from September 1992 to June 1983, and a visiting Assistant Professor at the Department of Statistics, Purdue University from September 1983 to May 1984. In June 1984 he has joined University of Tokyo, where he has been a Professor of Statistics with the Department of Mathematical Informatics since April 2001. He has served as President of Japan Statistical Society from January 2011 to June 2013. He has been working on multivariate distribution theory in statistics. Currently his main area of research is algebraic statistics. He also works on game-theoretic probability, which is a new approach to probability theory.

Satoshi Kuriki received the Bachelor and Ph.D. degrees from University of Tokyo, Japan, in 1982 and 1993, respectively. He is a Professor with the Institute of Statistical Mathematics (ISM), Tokyo, Japan, where he is also serving as Director of the Department of Mathematical Analysis and Statistical Inference. His current major research interests include geometry of random fields, multivariate analysis, multiple comparisons, graphical models, optimal designs, and genetic statistics.

Hyungdong Shin (S'01-M'04-SM'11) received the B.S. degree in electronics engineering from Kyung Hee University, Korea, in 1999, and the M.S. and Ph.D. degrees in electrical engineering from Seoul National University, Korea, in 2001 and 2004, respectively. During his postdoctoral research at the Massachusetts Institute of Technology (MIT) from 2004 to 2006, he was with the Wireless Communication and Network Sciences Laboratory within the Laboratory for Information Decision Systems (LIDS). In 2006, Dr. Shin joined Kyung Hee University, Korea, where he is now an Associate Professor at the Department of Electronics and Radio Engineering. His research interests include wireless communications and information theory with current emphasis on MIMO systems, cooperative and cognitive communications, network interference, vehicular communication networks, location-aware radios and networks, physical-layer security, molecular communications. Dr. Shin was honored with the Knowledge Creation Award in the field of Computer Science from Korean Ministry of Education, Science and Technology (2010). He received the IEEE Communications Society Guglielmo Marconi Prize Paper Award (2008) and William R. Bennett Prize Paper Award (2012). He served as a Technical Program Co-chair for the IEEE WCNC (2009 PHY Track) and the IEEE Globecom (Communication Theory Symposium, 2012). He was an Editor for IEEE Transactions on Wireless Communications (2007-2012). He is currently an Editor for IEEE Communications Letters.

Christoph Koutschan received the Master degree in Computer Science from Friedrich-Alexander University in Erlangen, Germany, and the Ph.D. degree in Symbolic Computation from the Johannes Kepler University in Linz, Austria. He worked as a researcher at the Research Institute for Symbolic Computation (RISC, Linz, Austria), at Tulane University (New Orleans, USA), and at INRIA (Institut national de recherche en informatique et en automatique, France). Currently he is with the Johann Radon Institute for Computational and Applied Mathematics (RICAM) of the Austrian Academy of Sciences. His research interests are on methods related to the holonomic systems approach, particularly symbolic summation and integration algorithms, and their application to problems from combinatorics, knot theory, special functions, numerical analysis, and statistical physics.